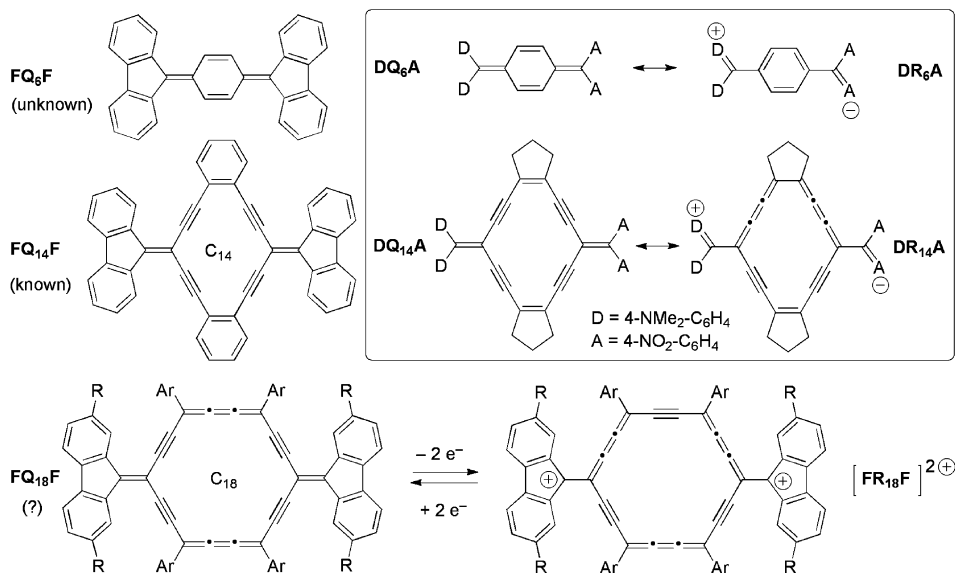


# Carbo-Quinoids: Stability and Reversible Redox-Proaromatic Character towards Carbo-Benzenes\*\*

Kévin Cocq, Valérie Maraval,\* Nathalie Saffon-Merceron, Alix Saquet, Corentin Poidevin, Christine Lepetit, and Remi Chauvin\*

**Abstract:** The carbo-mer of the para-quinodimethane core is stable within in a bis(9-fluorenylidene) derivative. Oxidation of this carbo-quinoid with  $\text{MnO}_2$  in the presence of  $\text{SnCl}_2$  and ethanol affords the corresponding *p*-bis(9-ethoxy-fluorenyl)-carbo-benzene. The latter can be in turn converted back into the carbo-quinoid by reduction with  $\text{SnCl}_2$ , thus evidencing a chemical reversibility of the interconversion between a pro-aromatic carbo-quinoid and an aromatic carbo-benzene, and is reminiscent of the behavior of the benzoquinone/hydroquinone redox couple (in the red-ox opposite sense).

Whereas quinones are stabilized by two strong C=O bonds, quinodimethanes (QDMs), possessing weaker C=C bonds, are more elusive species, in particular with respect to aromatization. While *ortho*-QDMs are thus transient tetraenes in synthetically valuable pericyclic processes,<sup>[1]</sup> the *para* isomers, such as tetracyano-QDM (TCNQ) in organic conductors, are prone to various redox processes.<sup>[2]</sup> Although functional *para*-QDMs can be handled as stable molecules,<sup>[3]</sup> only a few sensitive hydrocarbon



**Figure 1.** Illustration of the proaromaticity concept for push-pull quinoids based on 6- and 14-membered cores (top right), corresponding known and unknown bis(fluorenylidene) quinoids (top left), and envisaged redox generalization to carbo-quinoids (bottom).

representatives have been isolated,<sup>[4]</sup> and their reactivity is governed by their propensity to undergo aromatization to give benzene units. In a related context, the concept of proaromaticity has been developed by Diederich et al. for the analysis of the generation of aromaticity-stabilized electronic excited states through limited internal electron transfer in push-pull *p*-quinoids (**DQ<sub>6A</sub>**; Figure 1).<sup>[5a]</sup> the HOMO–LUMO gap is thus lowered through an increase of the ground-state level by charge pre-separation, which is balanced by linear delocalization between strong donor (**D**) and acceptor (**A**) ends, thus preventing cyclic delocalization in the aromatic ring of the minor zwitterionic form **DR<sub>6A</sub>**.<sup>[5]</sup>

Beyond proaromaticity toward 6 $\pi$ -electron benzene cores, a proaromatic dipolar *p*-quinoidic chromophore (**DQ<sub>14A</sub>**; Figure 1), based on a 14 $\pi$ -electron expanded radiannulenic core, was also devised.<sup>[5]</sup> It is noteworthy that the “proacetylenic” character of the two butatriene edges of the Kekulé structures **DR<sub>14A</sub>**,<sup>[6]</sup> or, equivalently, the generalized “aromatic character” of the four triple bonds,<sup>[7]</sup> may also help the molecule to resist complete aromatization.

A natural issue is whether the proaromaticity concept is generalizable to nonpolar molecules by reference to aromatic ionized ground states (oxidized or reduced) instead of electronic excited states.<sup>[5]</sup> The relevance of the corresponding “redox-proaromaticity” is addressed below for 9-fluorenyli-

[\*] K. Cocq, V. Maraval, A. Saquet, C. Poidevin, C. Lepetit, R. Chauvin CNRS, LCC (Laboratoire de Chimie de Coordination) 205 route de Narbonne, BP44099, 31077 Toulouse Cedex 4 (France)  
K. Cocq, V. Maraval, A. Saquet, C. Poidevin, C. Lepetit, R. Chauvin Université de Toulouse, UPS, ICT-FR 2599 31062 Toulouse Cedex 9 (France)  
E-mail: vmaraval@lcc-toulouse.fr  
chauvin@lcc-toulouse.fr

N. Saffon-Merceron Université de Toulouse, UPS Institut de Chimie de Toulouse ICT-FR-2599 118 route de Narbonne, 31062 Toulouse Cedex 9 (France)

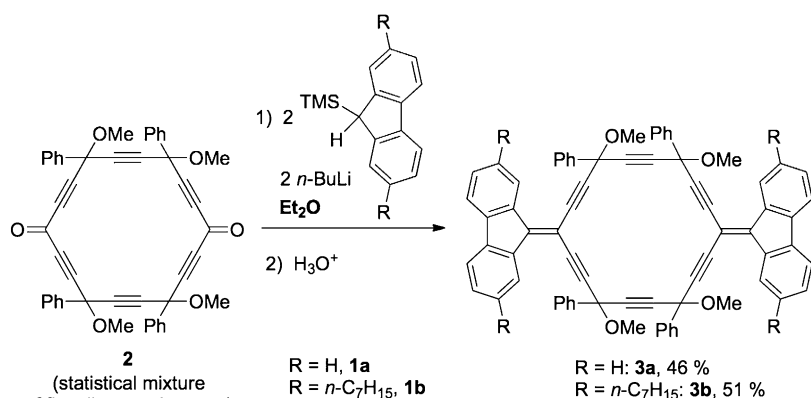
[\*\*] We thank the ANR program (ANR-11-BS07-016-01) for a doctoral fellowship for K.C. and for funding of equipment, along with the CNRS. We also thank Christian Bijani for NMR characterizations and Dr. Arnaud Rives for useful discussions and advice.



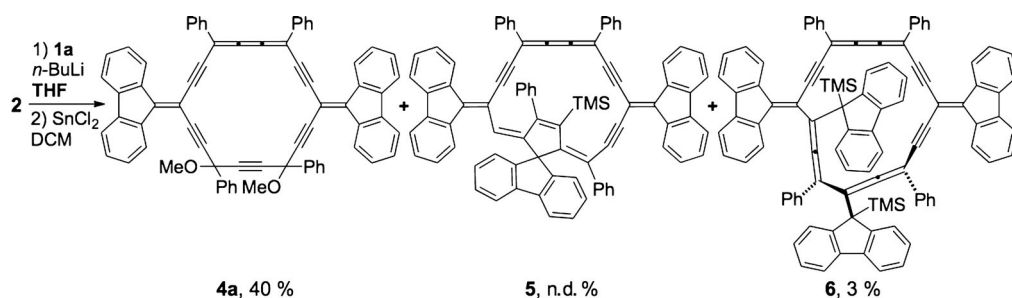
Supporting Information for this article is available on the WWW under <http://dx.doi.org/10.1002/ange.201407889>.

dene ends (**F**; Figure 1) and a sufficiently large core satisfying the  $4n+2$  Hückel rule. Whereas **FQ<sub>6</sub>F** escaped all attempts at isolation because of the strong aromaticity of the benzene ring ( $n=1$ ),<sup>[8]</sup> its *carbo-mer* **FQ<sub>18</sub>F** can be envisaged because of the weaker aromaticity of the *carbo*-benzene ring, for example, in the oxidized form [**FR<sub>18</sub>F**]<sup>2+</sup> ( $n=4$ ).<sup>[7]</sup> In the difluorenylidene  $[4n+2]$  quinoid series, the *carbo*-quinoid **FQ<sub>18</sub>F** is next after the term  $n=3$  exemplified by Tykewski et al. as **FQ<sub>14</sub>F**, where benzannulation guarantees the absence of macrocyclic aromatization.<sup>[9]</sup> In contrast, the C<sub>18</sub> *carbo*-benzene ring is definitely aromatic, but acyclic versions thereof are also stable.<sup>[10]</sup> These balancing factors make both the *carbo*-benzene **FR<sub>18</sub>F(OH)<sub>2</sub>** ( $=$  [**FR<sub>18</sub>F**]<sup>2+</sup>, 2OH<sup>−</sup>) and *carbo*-quinoid **FQ<sub>18</sub>F** a priori reasonable targets.

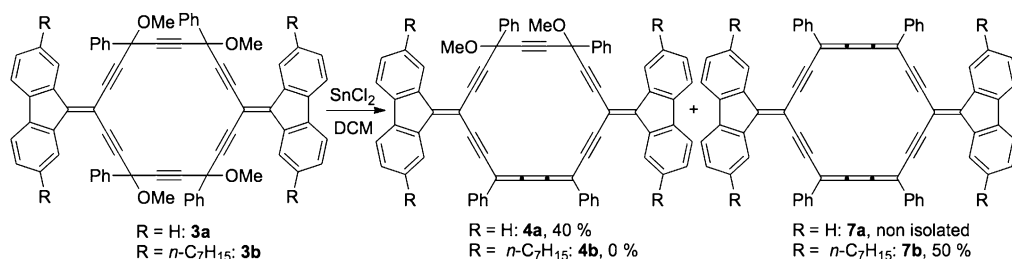
Two equivalents of the lithium salt of either 9-trimethylsilyl-9H-fluorene **1a**,<sup>[11]</sup> or the 2,7-dialkyl-homologue **1b**,<sup>[12]</sup> were thus added to the known [6]pericyclynedione **2** (Scheme 1).<sup>[13]</sup> In diethylether, the reaction cleanly afforded the difluorenylidene-[6]pericyclines **3a** (46%) and **3b** (51%). In THF, the reaction led to an intractable mixture, which, when treated with SnCl<sub>2</sub>, led to the partly reduced main product **4a**, along with small amounts of the dissymmetrical trifluorenylidene quinoid **5** and tetrafluorenylidene macrocyclic alleno-acetylenics **6**,<sup>[14]</sup> both identified by means of X-ray crystallography (Scheme 2 and the Supporting Information).<sup>[15]</sup>



**Scheme 1.** Synthesis of pericyclic precursors of difluorenylidene *carbo*-quinoids in Et<sub>2</sub>O. TMS = trimethylsilyl.



**Scheme 2.** Outcome of the reaction of a fluorenyllithium with the [6]pericyclynedione **2** in THF (XRD data of **5** and **6** in the Supporting Information).<sup>[15]</sup>



**Scheme 3.** Synthesis of the *carbo*-quinoids **7a,b** by treatment of **3a,b** with SnCl<sub>2</sub>. DCM = CH<sub>2</sub>Cl<sub>2</sub>.

Treatment of a pure sample of **3a** with SnCl<sub>2</sub> afforded the partly reduced product **4a** in 40% yield, while formation of the **FQ<sub>18</sub>F** prototype **7a** could not be evidenced (Scheme 3). Nevertheless, prolonged treatment of either **3a** or **4a** with SnCl<sub>2</sub> gave a blue precipitate, which was assigned as **7a** by MALDI-TOF MS ( $m/z$  852.3); insolubility prevented additional characterization. When applied to **3b**, the same treatment led, in 50% yield, to the soluble *carbo*-quinoid **7b**, which was stable (XRD molecular view in Figure 2).<sup>[15]</sup>

The conversion of **7b** into **8** (R = H) and **9** (R = Et) was triggered by treatment with MnO<sub>2</sub> in the presence of ROH, and SnCl<sub>2</sub> as a Lewis acid. The diethoxylated product **9** was found more stable than **8**, but both of them could be characterized by crystallography, in spite of the limited stability in the solid state.<sup>[15,16]</sup> <sup>1</sup>H NMR spectroscopy revealed a dramatic change in the electronic structure through the classical deshielding of the *ortho* <sup>1</sup>H nuclei of the phenyl substituents of the diatropic C<sub>18</sub> ring (from  $\delta$  = 8.04 ppm in **7b** to  $\delta$  = 9.41 ppm in **9**).<sup>[16]</sup>

Reduction of **9** to **7b** could also be performed by treatment with SnCl<sub>2</sub>. The *carbo*-quinoid to *carbo*-benzene interconversion can be monitored visually with the reaction medium evolving from blue to orange in about 15 minutes during the oxidation of **7b**, and from orange to blue in about 1.5 hours during the reduction of **9** (also affording polymerization side products).

While the UV-vis absorption spectrum of **9** is similar to those of other *carbo*-benzenes, with one intense band at  $\lambda_{\text{max}}$  = 454 nm

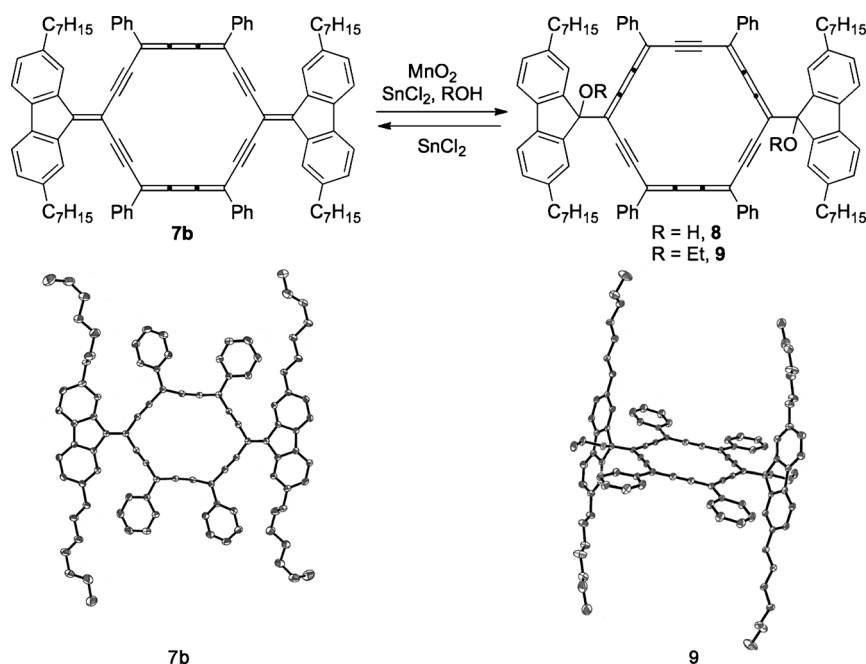


**Figure 2.** Reversible redox conversion of a *carbo*-quinoid into *carbo*-benzenes (top: only one of the equivalent Kekulé structures of **8** or **9** is depicted). XRD molecular views of **7b** (bottom, left), and **9** (bottom, right) (XRD data for **8** can be found in the Supporting Information).<sup>[15]</sup>

(Figure 3), the spectrum of **7b** displays two intense bands at  $\lambda = 435$  and  $591$  nm. The extinction coefficients of **9** at  $\lambda_{\text{max}}$  ( $\epsilon \geq 324\,400 \text{ L mol}^{-1} \text{ cm}^{-1}$ , estimated assuming that the conversion of **7b**  $\rightarrow$  **9** is quantitative, **9** being not stable enough to be dried and weighted precisely), is twice that of **7b** ( $\epsilon = 145\,500 \text{ L mol}^{-1} \text{ cm}^{-1}$ ). This pattern is reminiscent of the *carbo*-cyclohexadienes also featuring a conjugated but non-aromatic macrocyclic core between two identical ends.<sup>[16]</sup>

The pro-aromatic character of **7b** can be assessed by comparison of some of its aromaticity indices (structural, energetic, and magnetic criteria) with those of **8** or **9** (see the Supporting Information). Regarding the structural criterion, the standard deviation of the crystallographic bond lengths of the  $\text{C}_{18}$  ring is significantly larger in **7b** ( $0.090 \text{ \AA}$ ) than in **8** and

**9** [ $(0.075 \pm 0.001) \text{ \AA}$ ]. Regarding the energetic criterion, the electronic structure in the crystal geometry of **7b** and **9** was calculated at the B3PW91/6-31G\*\* level of theory on the model fragments **7c** and **9c**, which were obtained by truncation of the heptyl chains to methyl groups. The near-frontier out-of-plane  $\pi$  orbitals of **9c** are thus found to be much more localized on the  $\text{C}_{18}$  ring than those of **7c**, and the HOMO–LUMO gap is  $0.5 \text{ eV}$  smaller in **7c** than in **9c** (Figure 4).<sup>[16]</sup> Regarding the magnetic criterion, while the NICS(0) values of the  $\text{C}_{18}$  ring of **9c** and **7c** are calculated at  $-14.3 \text{ ppm}$  and  $+0.3 \text{ ppm}$ , respectively, the NICS(0) values of the phenyl substituents are shifted downfield in **7c** (ca.  $-4.5 \text{ ppm}$ ) with respect to **9c** (ca.  $-6.8 \text{ ppm}$ ). These data confirm the much higher macro-aromatic character of **9c** with respect to **7c** (see the Supporting Information for details).

Redox properties of **4a**, **7b**, and **9** were investigated by square-wave (SWV) and cyclic (CV) voltammetries

(Table 1 and the Supporting Information, all potentials given versus SCE). In the reduction process, four waves are observed for **4a** and **7b** and the first two are reversible at very close potentials ( $E_{1/2}$ :  $-0.74$  and  $-0.90 \text{ V}$  for **4a**,  $-0.67$  and  $-0.80 \text{ V}$  for **7b**), thus suggesting quasi-simultaneous reductions of the two remote exocyclic double bonds with the lower  $E_{1/2}$  values of **7b** being attributed to proaromaticity. With a classical *carbo*-benzene reduction comportment,<sup>[16]</sup> **9** is first reversibly reduced at  $-0.84 \text{ V}$ , then irreversibly at  $-1.30 \text{ V}$ . For the three compounds, an irreversible oxidation process occurs in the range  $1.14$ – $1.29 \text{ V}$ , and the products deposited on the electrode, as previously observed for *carbo*-benzenes.<sup>[16]</sup> The partly reduced product **4a** exhibits a second

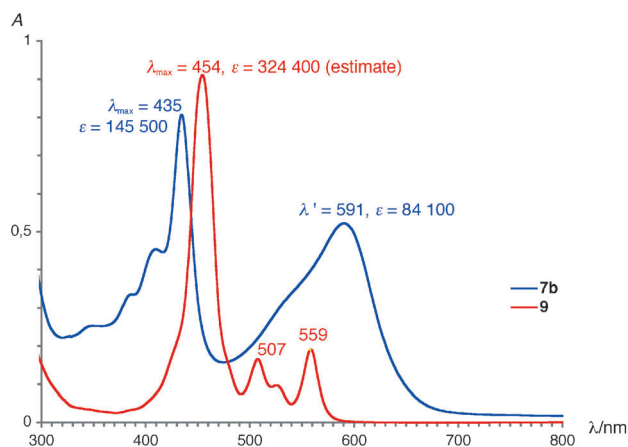


**Figure 3.** UV-vis spectra of the *carbo*-quinoid **7b** and *carbo*-benzene **9** in toluene ( $\epsilon$  values in  $\text{L mol}^{-1} \text{ cm}^{-1}$ ).

**Table 1:** CV data for **4a**, **7b**, and **9** on a Pt microdisk at RT in  $\text{CH}_2\text{Cl}_2$ ,  $0.1 \text{ M } [n\text{Bu}_4\text{N}][\text{PF}_6]$ ; SCE (reference); scan rate:  $0.2 \text{ Vs}^{-1}$ .

	$E_{1/2}^{[a]}$ [V]	$\Delta E_p$ [V] <sup>[b]</sup>	Reduction $R_f^{[c]}$	Number of $e^-$	Oxidation $E_p^{\text{ox}}$ [V]
<b>4a</b>	$-0.74$	$0.06$	$1.08$	2	$1.29^{[d]}$
	$-0.90$	$0.06$	$1.02$	2	$1.52$
					$-1.37$ $-1.75$
<b>7b</b>	$-0.67$	$0.06$	$1.00$	2	$1.14^{[d]}$
	$-0.80$	$0.05$	$1.10$	2	
	$-1.24$	$0.05$	$1.00$	2	$-1.53$
<b>9</b>	$-0.84$	$0.07$	$1.07$	–	$1.15^{[d,e]}$
					$-1.30$

[a] Half-wave potential  $E_{1/2} = (E_p^{\text{red}} + E_p^{\text{ox}})/2$ . [b] Separation between the two peak potentials:  $\Delta E_p = E_p^{\text{red}} - E_p^{\text{ox}}$ . [c] Peak current ratio  $R_f = |I_p^{\text{ox}}/I_p^{\text{red}}|$ . [d] The product deposited on the electrode. [e] Becomes reversible at high scan rates.

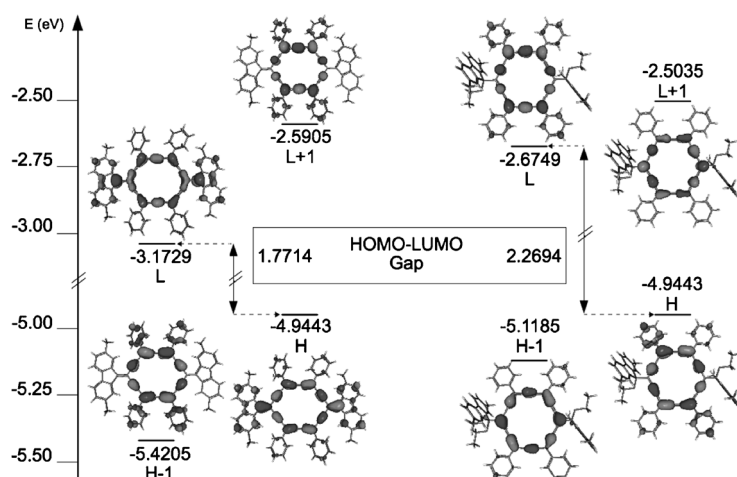


**Figure 4.** Orbital diagram of the *carbo*-quinoid **7c** (left) and *carbo*-benzene **9c** (right; B3PW91/6-31G\*\* level of calculation).

oxidation at 1.52 V, likely occurring at the dioxybutyne edge of the macrocycle.

Whereas the quinodimethane **FQ<sub>6</sub>F** escaped all attempts at isolation, its ring *carbo*-mer **7b** is stable, thus illustrating how *carbo*-merization can circumvent the instability of chemical prototypes. In passing, the redox proaromaticity of benzoquinone versus hydroquinone is shown to be relevant in the all-carbon series through the *carbo*-quinoid **7b** versus the *carbo*-benzenes **8** and **9**, albeit in the red-ox opposite sense. From these results, the *carbo*-mer of the benzoquinone/hydroquinone couple is thus a natural future target. Finally, as aromaticity accounts for valuable properties of  $\pi$ -extended organic molecular materials (chromophoric, optical, electrical or electrochemical), the reversible control of its setup with a minimal structural perturbation is a requirement for practical applications. This requirement is fulfilled by the redox interconversions between **7b** and **8, 9**, and these results open prospects for the design of chemical switches in future electro/optical devices.

Received: August 2, 2014

Revised: October 19, 2014

Published online: January 21, 2015

**Keywords:** alkynes · aromaticity · heterocycles · quinodimethanes · X-ray diffraction

- [1] M. Abe, *Chem. Rev.* **2013**, *113*, 7011–7088, and references therein.
- [2] D. S. Acker, W. R. Hertler, *J. Am. Chem. Soc.* **1962**, *84*, 3370–3374.
- [3] R. Gompper, H.-U. Wagner, E. Kutter, *Chem. Ber.* **1968**, *101*, 4123–4143.
- [4] S. Rosenfeld, S. Van Dyke, *J. Chem. Educ.* **1991**, *68*, 691–692.
- [5] a) Y.-L. Wu, F. Bures, P. D. Jarowski, W. B. Schweizer, C. Boudon, J.-P. Gisselbrecht, F. Diederich, *Chem. Eur. J.* **2010**, *16*, 9592–9605; b) J. L. Zafra, R. C. González Cano, M. C. Ruiz Delgado, Z. Sun, Y. Li, J. T. López Navarrete, J. Wu, J. Casado, *J. Chem. Phys.* **2014**, *140*, 054706.
- [6] Y.-L. Wu, F. Tancini, W. B. Schweizer, D. Paunescu, C. Boudon, J.-P. Gisselbrecht, P. D. Jarowski, E. Dalcana, F. Diederich, *Chem. Asian J.* **2012**, *7*, 1185–1190.
- [7] R. Chauvin, C. Lepetit, V. Maraval, L. Leroyer, *Pure Appl. Chem.* **2010**, *82*, 769–800.
- [8] a) B. J. Dahl, N. S. Mills, *J. Am. Chem. Soc.* **2008**, *130*, 10179–10186; b) J. Fabian, *Dyes Pigm.* **2010**, *84*, 36–53.
- [9] M. Gholami, M. N. Chaur, M. Wilde, M. J. Ferguson, R. McDonald, L. Echegoyen, R. R. Tykwinski, *Chem. Commun.* **2009**, 3038–3040.
- [10] A. Rives, V. Maraval, N. Saffon-Merceron, R. Chauvin, *Chem. Eur. J.* **2014**, *20*, 483–492, and references therein.
- [11] a) H. Hopf, H. Berger, G. Zimmermann, U. Nüchter, P. G. Jones, I. Dix, *Angew. Chem. Int. Ed. Engl.* **1997**, *36*, 1187–1190; *Angew. Chem.* **1997**, *109*, 1236–1238; b) S. W. Chang, J.-M. Hong, J. W. Hong, H. N. Choi, *Polym. Bull.* **2001**, *47*, 231–238.
- [12] Y. Ie, M. Endou, S. K. Lee, R. Yamada, H. Tada, Y. Aso, *Angew. Chem. Int. Ed.* **2011**, *50*, 11980–11984; *Angew. Chem.* **2011**, *123*, 12186–12190.
- [13] L. Leroyer, C. Zou, V. Maraval, R. Chauvin, *C. R. Chim.* **2009**, *12*, 412–429.
- [14] P. Rivera-Fuentes, F. Diederich, *Angew. Chem. Int. Ed.* **2012**, *51*, 2818–2828; *Angew. Chem.* **2012**, *124*, 2872–2882.
- [15] CCDC 1014356 (**5**), 1014357 (**6**), 1014358 (**7b**), 1029189 (**8**), and 1014359 (**9**) contain the supplementary crystallographic data for this paper. These data can be obtained free of charge from the Cambridge Crystallographic Data Centre via [www.ccdc.cam.ac.uk/data\\_request/cif](http://www.ccdc.cam.ac.uk/data_request/cif).
- [16] For examples, see: a) L. Leroyer, C. Lepetit, A. Rives, V. Maraval, N. Saffon-Merceron, D. Kandaskalov, D. Kieffer, R. Chauvin, *Chem. Eur. J.* **2012**, *18*, 3226–3240; b) A. Rives, I. Baglai, V. Malyskyi, V. Maraval, N. Saffon-Merceron, Z. Voitenko, R. Chauvin, *Chem. Commun.* **2012**, *48*, 8763–8765.